ORIGINAL PAPER

Novel approach using EIS to study flow accelerated pitting corrosion of AA5083-H321 aluminum–magnesium alloy in NaCl solution

K. Jafarzadeh · T. Shahrabi · A. A. Oskouei

Abstract EIS was utilized as a novel approach to study the role of mechanical and electrochemical processes in flow accelerated pitting corrosion behaviour of AA5083-H321 aluminum–magnesium alloy in 3.5% NaCl solution. This alloy is a suitable material for manufacturing of high speed boats, submarines, desalination systems etc. Impedance spectra were obtained during 24 h of exposure of the samples to the test solution at different rotation speeds. The surface and cross section of the samples were studied by scanning electron microscopy (SEM) and EDAX analysis. The results indicated that increasing the rotation speed causes the depth of pits to increase. By further increasing the rotation speed to 5 and 7 m s^{-1}, the flow condition causes the passive layer inside the pits to breakdown. Simultaneously, the thickness of the passive layer on the areas other than the pits becomes thinner. Shear stresses at 10 m s^{-1} are so severe that the passive layer on the entire surface breaks down and leads to micropitting corrosion.

Keywords Corrosion · AA5083-H321 aluminum–magnesium alloy · Impedance · Pitting · Flow

1 Introduction

Aluminum–Magnesium alloys have excellent resistance to corrosion in seawater. This is the main reason for their widespread use in the naval industry. In most naval applications, these alloys are exposed to severe hydrodynamic conditions [1, 2].

Pitting is one of the most common forms of corrosion in aluminum–magnesium alloys. The presence of heterogeneities, either in the metal or medium or in the exposure conditions, regardless of whether chloride is present or not, generally lead to this type of localized corrosion [3, 4]. Pitting corrosion occurs in the form of crevicing around the intermetallic particles because of microgalvanic coupling between the noble, iron-containing intermetallic particles and the surrounding more active solid solution aluminum matrix [5, 6].

Some researchers believe that increasing flow rates in seawater reduces the possibility of pitting observed in stagnant and low flow rate environments, while the rate of uniform corrosion increases [7, 8]. Davis and Ghering believe that under flowing conditions, due to disruption and removal of the oxide layer on particles of intermetallics, pitting corrosion occurs at those locations. Localized flow conditions on these pits and hydrodynamic shear stresses shear the particles off and remove the galvanic cell, leading to a decrease in the pitting corrosion rate. They also believe that the form and rate of corrosion of aluminum under hydrodynamic conditions depend on flow velocity [8, 9].

However, research by the authors showed that, at high speeds, pits covered a larger portion of the surface. It was also observed that high flow rate actually deepens the pits [10] and thus aggravates pitting corrosion.

The use of electrochemical impedance spectroscopy (EIS) for the study of corrosion processes has become extensive. This is because in principle this technique provides information relating to the different processes that simultaneously take place in any complex system [11, 12]. In previous work, EIS has been applied to study the process of pitting corrosion in aluminum alloys while the sample were exposed to stagnant NaCl solution [13, 14].

K. Jafarzadeh · T. Shahrabi (✉) · A. A. Oskouei
Material Engineering Department, Tarbiat Modares University, Tehran, Iran
e-mail: tshahrabi34@modares.ac.ir; kjafarzadeh@gmail.com

The aim of the present work is to use electrochemical impedance spectroscopy (EIS) to study the pitting corrosion mechanism of AA5083-H321 aluminum–magnesium alloy in NaCl solution under hydrodynamic conditions. This technique enables us to separate the role of electrochemical and mechanical factors in the pitting corrosion mechanism.

2 Experimental

The material studied was wrought aluminum–magnesium alloy AA5083-H321 with chemical composition given in Table 1.

Hydrodynamic conditions were provided by a rotating cylinder electrode (RCE) system. Cylindrical samples with 20 mm diameter and 15 mm height were used to conduct the different tests. The top and the bottom (circular faces) of the samples were painted off with two layers of epoxy [15], so that only the required surface of the samples was exposed to electrolyte. These samples were wet abraded with SiC paper down to 1500 grit and polished with alumina paste to 6 μm. Before use, the samples were degreased with acetone and then rinsed in distilled water. Room temperature NaCl solution of pH = 7 was used as test solution.

To de-aerate the solution it was purged with nitrogen gas 30 min prior to any test and this continued up to the end of the experiment.

Table 1 The chemical composition of AA5083-H321 alloy used for corrosion tests

Element	Mg	Si	Mn	Cr	Fe	Cu	Zn	Ti	Al
%weight	4.6	0.2	0.8	0.09	0.7	0.28	0.05	0.05	Balance
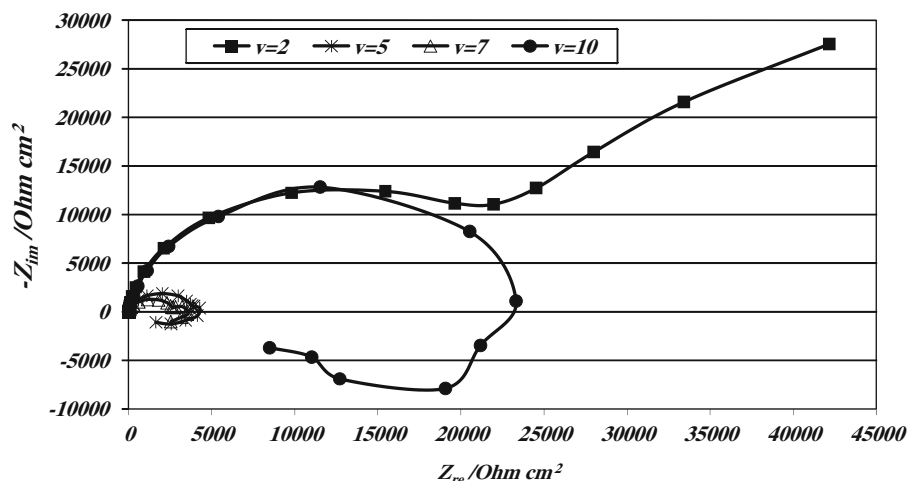
The impedance spectra were obtained using a Potentiostat/Galvanostat (EG&G Princeton Applied Research 273A) coupled to a model 1025 frequency response analyzer. The amplitude of the AC signal applied was ±10 mV, and the frequency ranged between 0.02 and 10^5 Hz. The equivalent circuits simulating the electrochemical response of the system were constructed making use of Zview2 software.

3 Results and discussion

Figure 1 shows the Nyquist plot for different rotation speeds of the sample in 3.5%wt NaCl solution. There is a difference between the Nyquist plots obtained at different rotation speeds. The plot at 2 m s^{-1} contains two capacitive loops at high and low frequencies. At 5 and 7 m s^{-1}, the plots included a capacitive loop at high frequencies, a capacitive loop at medium frequencies and an inductive loop at low frequencies. Finally, at 10 m s^{-1}, the plot only consists of a capacitive loop at high frequencies and an inductive loop at low frequencies.

Under the exposure condition studied here, two types of corrosion process take place in parallel. The first is the deterioration of zones of the matrix surrounding the precipitate present in the alloy as seen in Fig. 2a [16]. According to [17], the zone under EDAX analysis shown in Fig. 2b is more cathodic than that in the aluminum matrix. This makes the particles permanent cathodes and therefore the reduction of oxygen to hydroxyl ions occurs on these sites. This, in turn, produces a local increase in pH, giving rise to dissolution of the oxide layer in the area surrounding the precipitate. Once this layer has been dissolved, the local alkalisation causes an intense attack on the matrix. The evolution of this process over time can lead to the physical separation of the precipitate from the matrix, leading to the
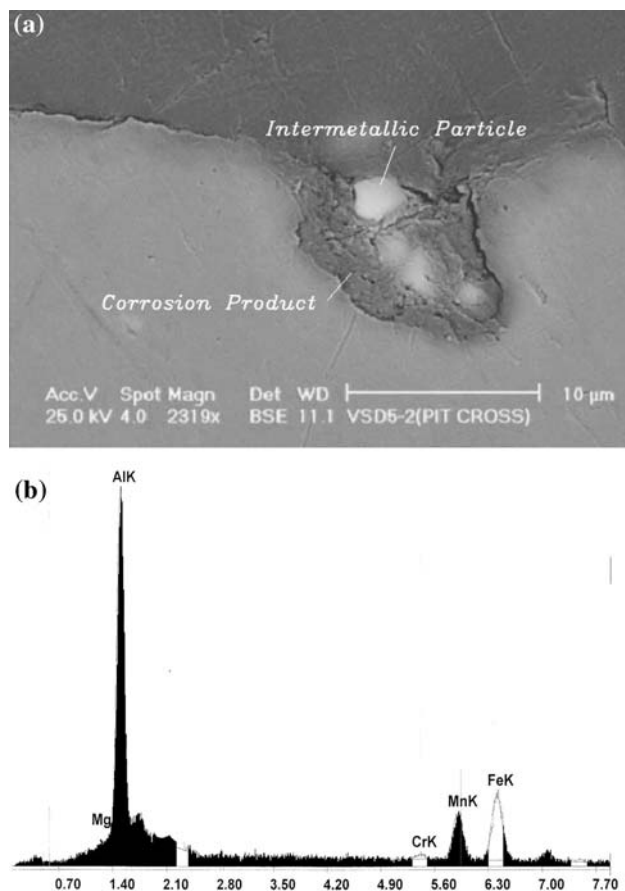
Fig. 1 Nyquist plot obtained on the surface at different rotation speeds

Fig. 2 a SEM image of cross section of the sample exposed in 3.5% NaCl solution after 24 h; **b** EDAX analysis of corrosion product inside the pit in **a**

formation of hemispherical pits which can be seen in Fig. 2a.

In addition to the process of alkaline corrosion just described, the matrix undergoes an oxidation process, which gives rise to the formation of a layer of alumina, the thickness of which increases with exposure time. This growth implies the existence of a process of transportation of Al^{+3} ions across this layer [18, 19]. The overall electrochemical response of the system will be the result of a combination of these processes. Consequently, the cross section of the sample can be represented schematically by Fig. 3a. Therefore, to produce the behaviour of the system in terms of an equivalent electrical circuit, the equivalent circuit in Fig. 3b is proposed which is consistent with the above mentioned explanations. In this equivalent circuit, CPE_{pit} and R_{pit} are the parameters related to the reactions inside the pit which cause galvanic corrosion between cathodic intermetallic particles and the matrix. C_l and R_l are also the parameters related to the growth of the passive layer. Figure 3c shows that there is a good compatibility between the experimental and simulated data. Table 2 reflects the effect of the exposure time on the activity of the

system. From Table 2, it can be confirmed that in passing from 1 to 6 h exposure, the values of R_{pit} and R_l decrease. This fall is related to acceleration of the galvanic reaction inside the pit. This leads to detachment of intermetallic particles from the pits and diminishing of cathodic reaction inside the pits. This is the reason for the increased values of R_{pit} after 12 h exposure, although the presence of other inter-metallic particle beneath the separated one causes the cathodic reaction to continue.

According to the mechanism presented, and referring to Eq. 1, the increase in T_{pit} will be related to the dissolution of the layer around the cathodic precipitates which causes an increase in the surface area of the matrix surrounding the precipitates.

By diminishing the cathodic reactions inside the pits, in parallel, the diffusion process across the passive layer become slower, leading to an increase in resistance across the passive layer, which manifests as an increase in the R_l value in Table 2.

Accepting the expression in Eq. 1, the fall in C_l after 6 h exposure time can be related to increased thickness of the passive layer covering the matrix [20].

$$C = \varepsilon\varepsilon_0 A d^{-1} \tag{1}$$

C, is the capacitance; ε, the dielectric permittivity; ε_0, the dielectric permittivity of vacuum; A, the surface area; D, the layer thickness.

Therefore, it can be concluded that although at 2 m s^{-1}, detachment of inter-metallic particles from the pit may cause the cathodic reaction to diminish, nevertheless, another inter-metallic particle at the bottom of pit can participate in further oxygen reduction. This results in the pit becoming deeper (Fig. 4).

To identify the reason for the appearance of an inductive loop at low frequencies in the Nyquist plot for rotation speeds of 5, 7 and 10 m s^{-1}, the test was also conducted in deaerated solution. This indicates that the observed inductive loop in Fig. 1 is due to the adsorption of oxygen anions at the substrate. Therefore, this behaviour can be attributed to breakdown of the passive layer on the sample either inside the pits or all over the surface (Fig. 5). It has been shown that flow conditions inside the pits create more intense shear stresses in comparison with other areas on the surface [21].

The equivalent circuit in Fig. 6a was proposed to reproduce the behaviour of the system at 5 and 7 m s^{-1} rotation speeds. In this circuit, T_{pit}, R_{pit} and L_{pit} are the parameters related to the reactions inside the pits, C_l and R_l are the parameters related to the diffusion through the passive layer on the surface and W_T is the Warburg coefficient at the Nernst layer adjacent to the surface. Oxygen should diffuse through this layer to reach the surface of the sample.

Fig. 3 **a** Schematic representation from the cross sectional view of aluminum–magnesium alloys; **b** Equivalent circuit simulated to electrical elements in **a**; **c** Good compatibility between simulated and experimental data in Nyquist plot of the sample at rotation speed of 2 m s^{-1}
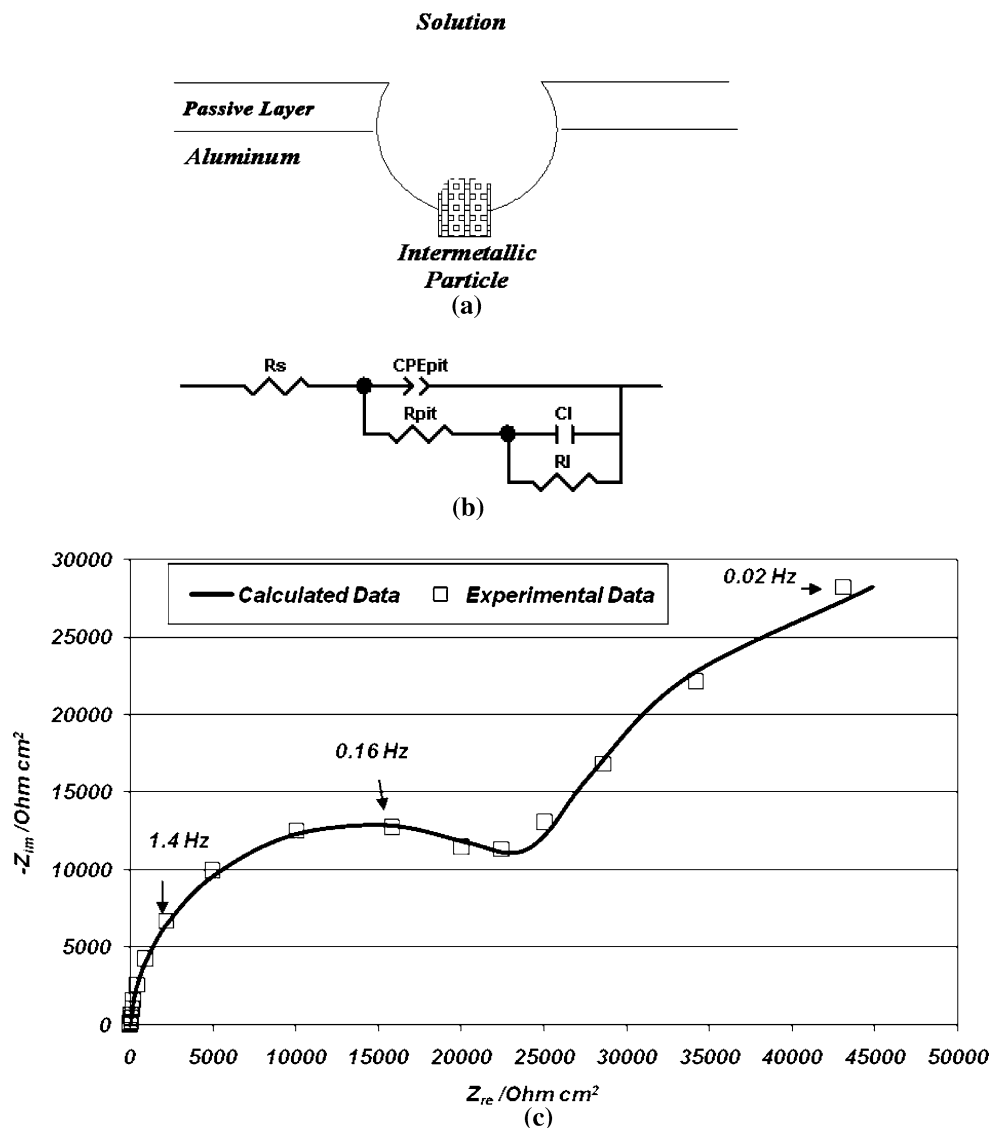

Table 2 Values of elements of the equivalent circuit fitted to the spectra obtained in 3.5% NaCl solution at rotation speed of 2 m s^{-1}

Time (h)	R_{pit} (ohm cm^2)	T_{pit} (μF cm^{-2} s^{n-1})	n_{pit}	R_l (ohm cm^2)	C_l (μF cm^{-2})
1	19600	7.4	0.92	70800	190
3	17700	8.2	0.95	70493	250
6	16600	9.6	0.95	47198	260
12	27770	10	0.95	54445	180
24	32433	12	0.95	62391	175

Table 3 reflects the effect of the exposure time on the activity of the system at a rotation speed of 5 m s^{-1}. The data obtained at 7 m s^{-1} are similar to those for 5 m s^{-1}.

The decrease in R_{pit} and the increase in T_{pit} with the time of exposure is related to an increase in active surface inside the pits. This is the result of both the electrochemical activity between the intermetallic particles and the matrix on the one hand and breakdown of passivity by shear stresses inside the pits on the other.

Referring to Eq. 1 it can be deduced that C_l decreases in accordance with the mechanism presented for passive layer growth at a rotation speed of 2 m s^{-1}. The increase in C_l and decrease in R_l in Table 3 reflects a phenomenon other than that observed in the case of 2 m s^{-1}. This behaviour can only originate from the decrease in thickness of the passive layer on the sample. Therefore, it can be concluded that the relative velocity between the sample and the solution can cause erosion corrosion on the sample, which
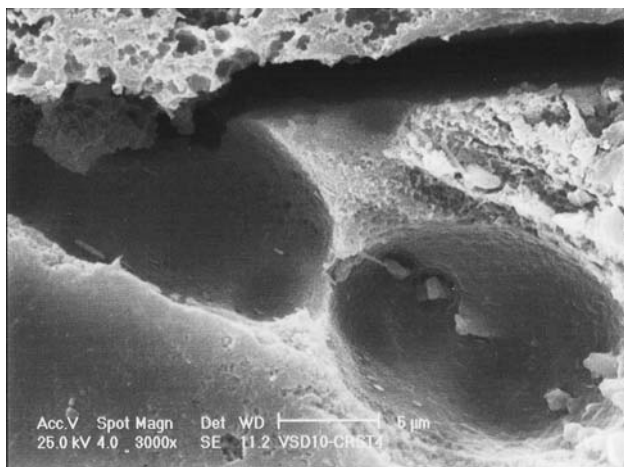
Fig. 4 Increase in depth of pit by exposing the new intermetallic particles to the solution

results in mechanical removal of the passive layer. Therefore, it can be inferred that at 5 and 7 m s^{-1} rotation speeds, pits are deepened by mechanical breakdown of the passive layer inside the pits. Variation of L_{pit} in Table 3 supports this conclusion. Larger surface area inside the pits causes the L_{pit} to increase in accordance with Eq. 2 in which [22]:

$$L = \mu_0 \mu_T N^2 A / l \qquad (2)$$

L, is the inductance; μ_0, the permitivity in vaccum; μ_T, the core material permitivity; N, the coil number; A, the cross sectional area of the coil; L, the coil length.

In parallel, erosion corrosion in areas other than the pits decreases the thickness of the passive layer.

The Nyquist representation of the impedance response of the alloy AA5083-H321 at a rotation speed of 10 m s^{-1} is shown in Fig. 7. Figure 7 shows only one capacitive loop at high frequencies and an inductive loop at low frequencies.
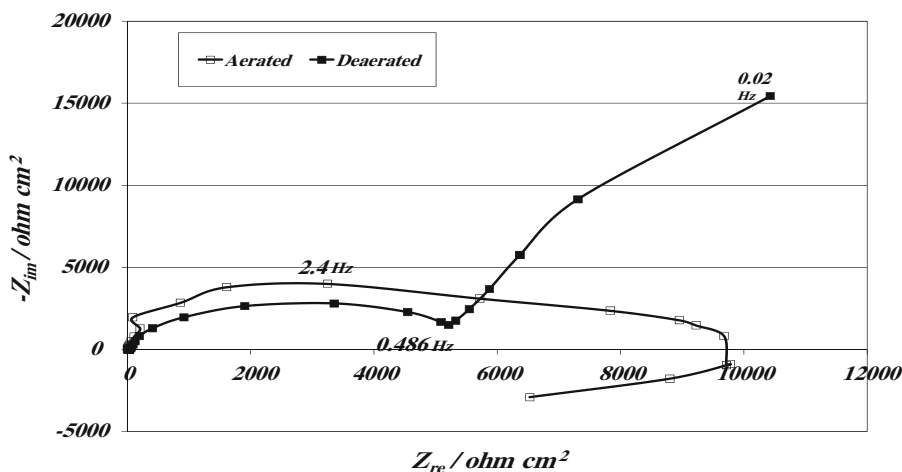
This means that one of the time constants (pit or passive layer), which had been previously seen in the Nyquist plots at 5 and 7 m s^{-1}, has been removed at this rotation speed. From Fig. 7, it can be observed that the pits are present on the surface even at a rotation speed of 10 m s^{-1}. This suggests that the passive layer might have been removed from the surface completely. By eliminating the parameters related to the passive layer from the equivalent circuit in Fig. 6a, we obtain the equivalent circuit shown in Fig. 8a. Figure 8b shows that there is good compatibility between the experimental and simulated data based on the proposed equivalent circuit in Fig. 8a. Therefore, it can be concluded that shear stresses on the surface, which caused a decrease in thickness of the passive layer on the surface at rotation speeds of 5 and 7 m s^{-1}, can completely remove this layer at a rotation speed of 10 m s^1. This provides a clue to the conditions necessary for incorporation of submicron sized intermetallic particles that appear in pitting corrosion and which are seen in micropits in Fig. 7.

The data obtained for different exposure times at a rotation speed of 10 m s^{-1} are shown in Table 4. Similar variations of parameters such as R_{pit} and T_{pit} to that in Table 3, indicate that the pit enlargement mechanism at this speed is similar to that seen at 5 and 7 m s^{-1}.

It was observed in Tables 2, 3 and 4 that the values of R_{pit} and T_{pit} do not show much difference. On the other hand, the cathodic limiting current density, which is responsible for cathodic reactions between intermetallic particles and the matrix inside the pits, is almost the same for rotation speeds of 5 m s^{-1} or more [10]. Therefore, by increasing the rotation speed of the sample to more than 5 m s^{-1}, there is no obvious change in electrochemical processes on the surface. However, mechanical processes (erosion corrosion) become more effective.

From Table 4 it can be seen that the values of R_l and L_l do not follow an established trend. This means that

Fig. 5 Nyquist plot obtained at aerated and deaerated solution at rotation speed of 7 m s^{-1}

Fig. 6 a Equivalent circuit proposed to reproduce the response of the system at rotation speeds of 5 and 7 m s^{-1}. **b** Good compatibility between simulated and experimental data in Nyquist plot of the sample after 24 h
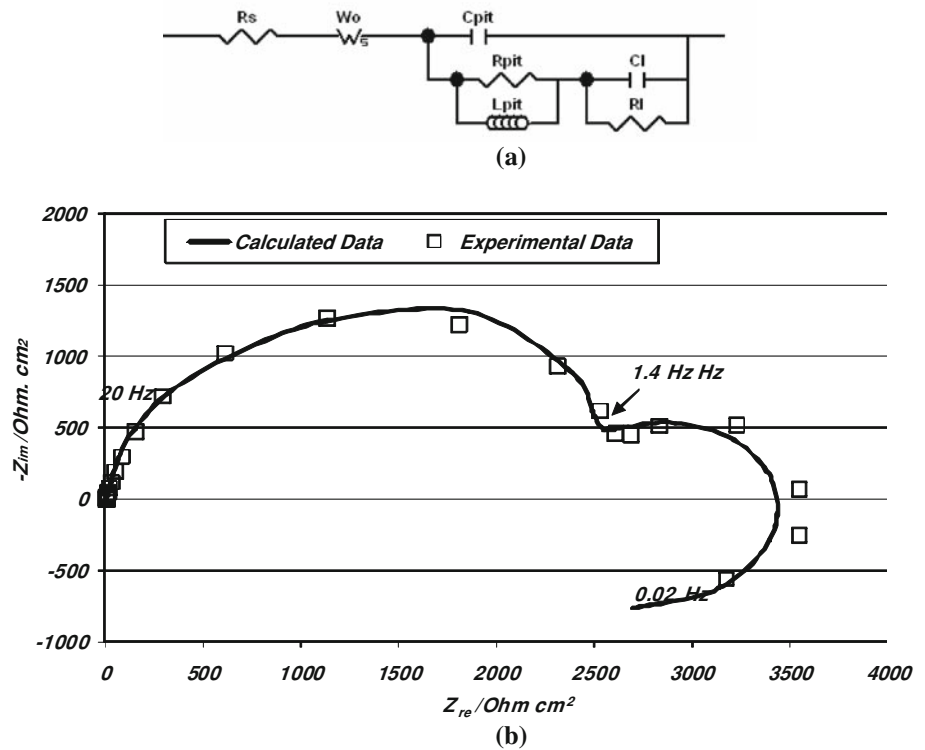

(a)

(b)

Table 3 Values of elements of the equivalent circuit fitted to the spectra obtained in 3.5% NaCl solution at rotation speed of 5 m s^{-1}

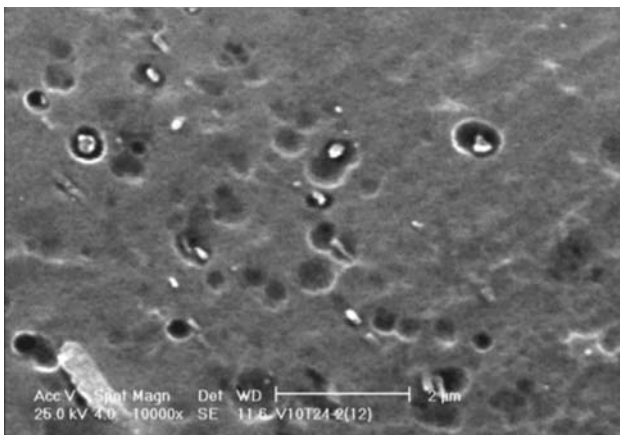| Time (h)	W_T	R_{pit} (ohm cm^2)	C_{pit} (µF cm^{-2})	L_{pit} (H cm^2)	R_l (ohm cm^2)	C_l (µF cm^{-2})
3	0.1	12512	8.3	74158	10115	63
6	0.12	4752	8.5	25047	1687	230
12	0.12	2746	10	10905	1369	555
24	0.11	2375	12	13231	739	690

Fig. 7 Micro pits on the surface of the sample at rotation speed of 10 m s^{-1}

erosion corrosion has caused the passive layer, which may be formed by adsorption of oxygen anions on the surface, to break down, possibly due to shear stresses.

In addition, equal values of W_T for rotation speeds of 5 m s^{-1} and more, is another reason for the values of R_{pit} and C_{pit} to be close to each other. Because oxygen, which is essential for cathodic reaction on intermetallic particles, should pass through the Nernst layer adjacent to the sample in accordance with Eq. 3, the value of l does not differ so much [23].

$$W_T = L^2/D \qquad (3)$$

D, is diffusion coefficient; L, the diffusion layer thickness (Nernst layer).

Fig. 8 **a** Equivalent circuit proposed to reproduce the response of the system at rotation speed of 10 m s^{-1}. **b** Good compatibility between simulated and experimental data in Nyquist plot of the sample after 24 h
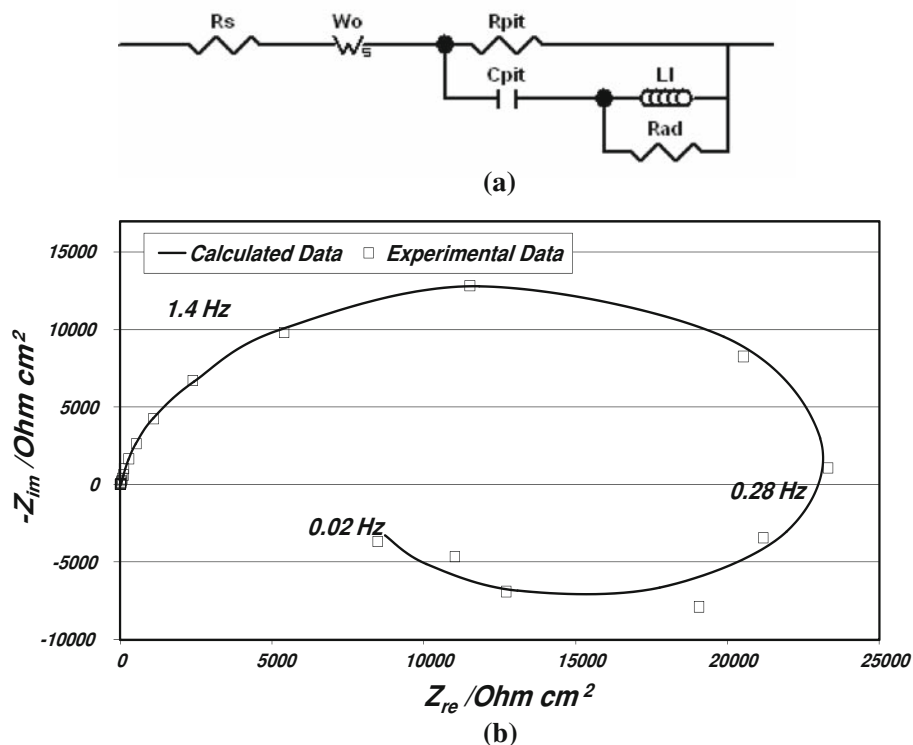

(a)

(b)

Table 4 Values of elements of the equivalent circuit fitted to the spectra obtained in 3.5% NaCl solution at rotation speed of 10 m s^{-1}

Time (h)	W_T	R_{pit} (ohm cm^2)	C_{pit} (μF cm^{-2})	L_l (H cm^2)	R_l (ohm cm^2)
3	0.08	4276	7.1	27431	2452
6	0.09	3696	9.9	95620	22037
12	0.08	3466	10.7	27730	15192
24	0.07	2194	12	14749	6850

4 Conclusion

EIS analysis of pitting corrosion on samples at different rotation speeds showed that increasing rotation speed causes mechanical processes to overcome the effect of electrochemical reactions. Thus at a rotation speed of 2 m s^{-1} the main process is acceleration of cathodic reaction inside the pits and growth of the passive layer on the surface. With increase of the rotation speed to 5 and 7 m s^{-1}, shear stresses cause the passive layer inside the pits to break down and the thickness of the passive layer on the areas other than the pits to decrease.

At a rotation speed of 10 m s^{-1} this condition becomes so severe that the passive layer on the entire surface breaks down and causes micropitting.

References

1. Chester HH (1985) Mar Technol 22:155
2. Brown S (1994) Feasibility of replacing structural steel with aluminum alloy s in shipbuilding industry. Report Published by University of Viscontin at Madison
3. Davis JR (1999) Corrosion of aluminum and aluminum alloys. ASM International, Materials Park, OH
4. Bethencourt M, Botana FJ (1998) Mater Sci Forum 289–292:567
5. Barbucci A, Bruzzone G (2000) Intermetallics 8:305
6. Birbilis N, Buchheit RG (2005) J Electrochem Soc 152:140
7. Nisancioglu K (2004) Corrosion and protection of aluminum alloys in seawater, Eurocorr 2004
8. Ghering GA, Peterson MH (1981) Corrosion 37:232
9. Davis JA, Ghering GA (1975) Mater Perform 4:87
10. Jafarzadeh K, Shahrabi T, Hosseini MG et al (2007) J Mater Sci Technol 23:623
11. Mansfeld F (1990) Electrochim Acta 35:1533
12. Macdonald DD (2006) Electrochim Acta 51:1376
13. Silverman DC, Carrico JE (1988) Corrosion 44:280
14. Aballe A, Bethencourt M, Botana FJ (2001) Mater Corros 53:185
15. SSPC Standards, systems and specifications (1995) Edited by Janes Rex 112
16. De Wit JH, Lenderink HJW (1996) Electrochim Acta 41:1111
17. Smialowska ZS (1999) Corros Sci 41:1743
18. Aballe A, Bethencourt M, Botana FJ et al (2001) Corros Sci 43:1657
19. Aballe A, Bethencourt M, Botana FJ et al (2003) Corros Sci 45:161
20. Frers SE, Stefenel MM, Mayer C et al (1990) J Appl Electrochem 20:996
21. Jafarzadeh K, Shahrabi T, Hosseini MG et al (2008) J Mater Sci Technol 24:215
22. http://www.electronics-tutorials.com/basics/Inductance (2007)
23. Juttner K (1990) Electrochim Acta 35:1501